Structure and Mesomorphic Behavior of Alkoxy-Substituted Bis(phthalocyaninato)lanthanide(III) Complexes

Koen Binnemans,*,† Jurgen Sleven,† Steven De Feyter,† Frans C. De Schryver,† Bertrand Donnio,‡ and Daniel Guillon‡

Department of Chemistry, Katholieke Universiteit Leuven, Celestijnenlaan 200F, B-3001 Leuven, Belgium, and Institut de Physique et Chimie des Matériaux de Strasbourg—Groupe Matériaux Organiques, UMR 7504 CNRS-Université Louis Pasteur, BP 43, 23 rue du Loess, F-67034 Strasbourg Cedex 2, France

Received April 4, 2003. Revised Manuscript Received June 30, 2003

The influence of the lanthanide ion and the chain length on the thermal properties of bis[2,3,9,10,16,17,23,24-octakis(alkoxy)phthalocyaninato]lanthanide(III) complexes, denoted in the following as $[(C_nH_{2n+1}O)_8Pc]_2Ln$, have been investigated. Two series of complexes were considered: a first series in which the alkoxy chain was kept constant with different lanthanide ions (Ln = Pr, Nd, Eu, Gd, Tb, Dy, Ho, Er, Tm, Yb, Lu), namely, $[(C_{12}H_{25}O)_8Pc]_2Ln$, and a second series of bis(phthalocyaninato)erbium(III) double-deckers, $[(C_nH_{2n+1}O)_8Pc]_2Er$, with different alkoxy chain lengths (n = 4−18). All these metallomesogens exhibit a hexagonal columnar mesophase (Col_h) over wide temperature ranges. It was found that the transition temperatures were not affected to a great extent by the lanthanide ion and that they could be tuned by a proper choice of the alkoxy chain length. The orientational behavior of $[(C_{12}H_{25}O)_8Pc]_2Er$ in contact with a substrate has also been investigated by scanning tunneling microscopy.

1. Introduction

The first lanthanide-containing liquid crystals were the bis[2,3,9,10,16,17,23,24-octakis(alkoxymethyl)phthalocyaninato]lutetium(III) complexes $[(C_nH_{2n+1}OCH_2)_8Pc]_2Lu$ (n = 8, 12, 18) described by Piechocki et al. in 1985.[1] Since then, relatively few papers have been published on this class of metallomesogens, and moreover most studies of liquid-crystalline Pc_2Ln sandwich complexes have been restricted to Lu^{III} as the central metal ion.[2] Besides alkoxymethyl-substituted complexes,[1,3] bis(phthalocyaninato)lanthanide(III) complexes with alkyl,[4,5] alkoxy,[6−12] alkylthio,[13,14] and poly(oxyethylene) chains[15] have been reported. Such complexes are of interest for their potential use in molecular electronics, and particularly as one-dimensional molecular semiconductors.[16,17] Indeed, monodomains of perfectly aligned columnar mesophases formed by such metallophthalocyanines can be considered as electrical wires at a molecular level, the molten alkyl chains acting as insulating shells.

To investigate the influence of the lanthanide ion and the chain length on the thermal properties of liquid-crystalline bis(phthalocyaninato)lanthanide(III) complexes, we prepared two series of octakis(alkoxy)-substituted compounds: a first series of double-deckers $[(C_{12}H_{25}O)_8Pc]_2Ln$ with different lanthanide ions and a series $[(C_nH_{2n+1}O)_8Pc]_2Er$ with different alkoxy chains (Figure 1). All the new sandwich complexes described here exhibited a hexagonal columnar mesophase (Col_h) over broad temperature ranges, that is, 100−150 °C. In this systematic study, it was found that the nature of the lanthanide ion has only a limited influence on the transition temperatures, and particularly the melting

* Corresponding author: Fax: +32 16 32 7992. E-mail: Koen.Binnemans@chem.kuleuven.ac.be.
† Katholieke Universiteit Leuven.
‡ UMR 7504 CNRS-Université Louis Pasteur.

(1) Piechocki, C.; Simon, J.; André, J. J.; Guillon, D.; Petit, P.; Skoulios, A.; Weber, P. *Chem. Phys. Lett.* **1985**, *122*, 124.
(2) Binnemans, K.; Görller-Walrand, C. *Chem. Rev.* **2002**, *102*, 2303.
(3) Piechocki, C. Matériaux Moleculaires a Base de Phthalocyanines Substituées Cristalline Liquides. Ph.D. Thesis, Université Pierre et Marie Curie−Paris VI, France, 1985.
(4) Komatsu, T.; Ohta, K.; Fujimoto, T.; Yamamoto, I. *J. Mater. Chem.* **1994**, *4*, 533.
(5) Komatsu, T.; Ohta, K.; Watanabe, T.; Ikemoto, H.; Fujimoto, T.; Yamamoto, I. *J. Mater. Chem.* **1994**, *4*, 537.
(6) Belarbi, Z.; Sirlin, C.; Simon, J.; André, J. J. *J. Phys. Chem.* **1989**, *93*, 8105.
(7) van de Craats, A. M.; Warman, J. M.; Hasebe, H.; Naito, R.; Ohta, K. *J. Chem. Chem. B* **1997**, *101*, 9224.
(8) Sleven, J.; Binnemans, K.; Görller-Walrand, C. *Mater. Sci. Eng. C* **2001**, *18*, 229.
(9) Naito, R.; Ohta, K.; Shirai, H. *J. Porphyrins Phthalocyanines* **2001**, *5*, 44.
(10) Maeda, F.; Hatsusaka, K.; Ohta, K.; Kimura, M. *J. Mater. Chem.* **2003**, *13*, 243.
(11) Liu, W.; Jiang, J. Z.; Pan, N.; Arnold, D. P. *Inorg. Chim. Acta* **2000**, *310*, 140.
(12) Jiang, J. Z.; Liu, R. C. W.; Mak, T. C. W.; Chan, T. W. D.; Ng, D. K. P. *Polyhedron* **1997**, *16*, 515.
(13) Ban, K.; Nishizawa, K.; Ohta, K.; van de Craats, A.; Warman, J. M.; Yamamoto, I.; Shirai, H. *J. Mater. Chem.* **2001**, *11*, 321.
(14) Yoshino, K.; Lee, S. B.; Sonoda, T.; Kawagishi, H.; Hidayat, R.; Nakayama, K.; Ozaki, M.; Ban, K.; Nishizawa, K.; Ohta, K.; Shirai, H. *J. Appl. Phys.* **2000**, *88*, 7137.
(15) Toupance, T.; Bassoul, P.; Mineau, L.; Simon, J. *J. Phys. Chem.* **1996**, *100*, 11704.
(16) McKeown, N. B. in *Phthalocyanine Materials: synthesis, structure, function*; Cambridge University Press: Cambridge, 1998.
(17) Simon, J.; Bassoul, P. *Design of Molecular Materials; Supramolecular Engineering*; Chichester: Wiley, 2000.

10.1021/cm034236o CCC: $25.00
Published on Web 08/28/2003

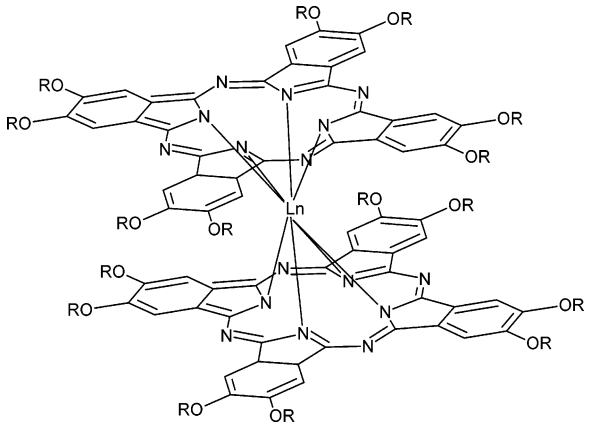

Figure 1. Structure of an alkoxy-substituted bis(phthalocyaninato)lanthanide(III) complex $[(RO)_8Pc]_2Ln$, where $R = C_nH_{2n+1}$.

temperature into the mesophase whereas they could be tuned by a proper choice of the alkoxy chain length. STM images of $[(C_{12}H_{25}O)_8Pc]_2Er$ deposited on various substrates have been recorded and compared to those of the corresponding metal-free phthalocyanine $(C_{12}H_{25}O)_8PcH_2$.

2. Experimental Section

2.1. Techniques. Elemental analyses (CHN) were performed on a CE-Instrument EA-1110 elemental analyzer. Mass spectra of the organic precursors were recorded on a low-resolution electron-impact Hewlett-Packard 5989A for low molecular mass substances. MALDI-TOF mass spectra of the phthalocyanine complexes were measured on a VG Tofspec SE (Micromass, UK) equipped with a N_2 laser (337 nm). IR spectra were obtained on a Bruker IFS66 FTIR spectrometer. The KBr-pellet technique was used to measure the samples. Differential scanning calorimetry (DSC) measurements were performed on a Mettler-Toledo DSC822e module (scan rate 10 °C min^{-1} under a helium flow, aluminum cups). Optical textures of the mesophases were observed using an Olympus BX60 polarizing microscope equipped with a Linkam THMS600 hot stage and a Linkam TMS93 programmable temperature controller. The powder XRD patterns were obtained with two different experimental setups, and the crude sample was filled in Lindemann capillaries (diameter: 1 mm). A linear monochromatic Cu $K\alpha_1$ beam ($\lambda = 1.5405$ Å) was obtained with a sealed-tube generator (900 W); a Guinier camera and a Debye−Scherrer camera equipped with a bent quartz monochromator and an electric oven were used. In both setups the temperature was controlled within ±0.3 °C. A first set of diffraction patterns was registered with a curved counter "Inel CPS 120" associated with a data acquisition computer system; periodicities up to 60 Å can be measured. The other set of diffraction patterns was registered on an image plate; periodicities up to 90 Å can be measured. The phase symmetry was then determined and the cell parameter, a, as well as the columnar cross-section, S, were calculated from the position of the most intense reflections at the smallest Bragg angle according to the equations $a = (2/[3\sqrt{3}])(d_{10} + \sqrt{3}d_{11} + 2d_{20})$ and $S = (\sqrt{3}/2)a^2$, respectively. In each case, exposure times were varied from 1 to 4 h.

Prior to STM imaging, all compounds under investigation were dissolved in 1-phenyloctane and a drop of this solution was applied on a freshly cleaved surface of highly oriented pyrolytic graphite (HOPG). The STM images were acquired in the variable current mode (constant height) under ambient conditions with the tip immersed in the liquid. In the acquired STM images, the brighter the features, the higher the measured tunneling current. STM experiments were performed using a Discoverer scanning tunneling microscope (Topometrix Inc., Santa Barbara, CA) along with an external pulse/function generator (Model HP 8111 A), with negative sample bias. Tips were electrochemically etched from Pt/Ir wire (80%/20%, diameter 0.2 mm) in a 2 N KOH/6 N NaCN solution in water.

Scheme 1. Synthesis of the $[(RO)_8Pc]_2Ln$ Complexes ($R = C_nH_{2n+1}$)[a]

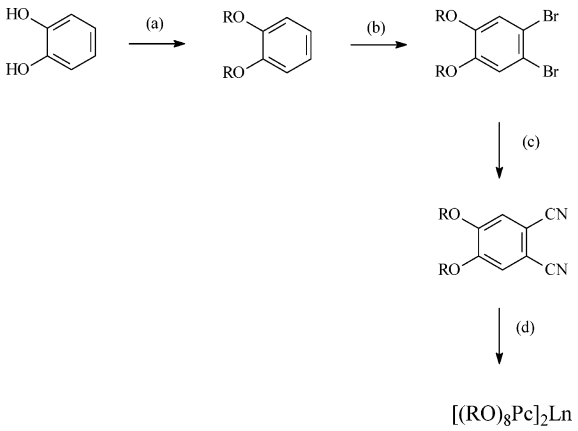

[a] Experimental conditions: (a) RBr, KOH, Aliquat 336; (b) Br_2, DCM; (c) CuCN, DMF; (d) $Ln(OAc)_3 \cdot nH_2O$ (1/8 equiv), DBU (1/2 equiv), 1-pentanol.

The experiments were repeated in several sessions using different tips to check for reproducibility and to avoid artifacts. The setpoint current and the sample bias voltage are indicated in figure captions. After registration of a STM image of a monolayer structure, the underlying graphite surface was recorded at the same position by decreasing the bias voltage, serving as an in situ calibration. All STM images contain raw data and are not subjected to any manipulation or image processing. The synthesis of $(C_{12}H_{25}O)_8PcH_2$ has been described in ref 8.

2.2. Synthesis of the 1,2-Dicyano-4,5-bisalkoxy Benzene Precursors. To study the effect of the chain length on the mesomorphic behavior of the phthalocyanine complexes, the complete series of 1,2-dicyano-4,5-bisalkoxybenzenes with chain lengths ranging from OC_4H_9 to $OC_{18}H_{37}$ was synthesized (Scheme 1).[8,18] The synthesis of the bis(alkoxy)benzenes was done by means of a Williamson ether synthesis, via a phase transfer mechanism: a mixture of catechol, the appropriate 1-bromoalkane, the base (KOH), and a catalytic amount of Aliquat 336 was heated for 3 h at 120 °C under a nitrogen atmosphere. 1-Bromo-octadecane ($C_{18}H_{37}Br$) being a solid at room temperature was melted prior to the addition of the other reactants. Purification of the 1,2-dicyano-4,5-bisalkoxybenzenes was done by crystallization from acetone. Most products were pure after one crystallization (the purity was checked by ^1H NMR, CHN analysis, and thin-layer chromatography, TLC). For a number of shorter chain lengths (OC_4H_9 to OC_8H_{17}), the reaction products were obtained as liquid and were purified by vacuum distillation.

The Williamson synthesis was followed by the bromination of the 1,2-dialkoxybenzene in the 4- and 5-positions. The product was dissolved in dichloromethane and placed in an ice bath. A solution of bromine in dichloromethane was slowly added, and after its complete addition, the mixture was stirred for 2 additional hours. The organic layer was washed with a saturated sodium metabisulfite solution, then with a saturated sodium hydrogen carbonate solution, and finally with water. After drying and evaporation of the solvent, the product was purified by crystallization from acetone. For some compounds, TLC gave evidence of the presence of monobrominated product. In this case, the compound was brominated a second time with an appropriate equivalent amount of bromine and the reaction mixture was purified by column chromatography on silica gel with an ethyl acetate−hexane mixture. The liquid dibromi-

(18) van der Pol, J. F.; Neeleman, E.; Zwikker, J. W.; Nolte, R. J. M.; Drenth, W. *Trav. Chim. Pays-Bas* **1988**, *107*, 615.

nated bisalkoxybenzenes (OC_4H_9 and OC_6H_{13}) were purified in an analogous manner.

The Rosenmund−Von Braun reaction consisted of refluxing the 1,2-dibromo-4,5-bis(alkoxy)benzenes in dimethylformamide (DMF) for 6 h under a nitrogen atmosphere in the presence of a slight excess of CuCN (ratio CuCN/dibrominated product = 2:7). After cooling to room temperature, the mixture was poured into an aqueous ammonia solution and the solution was stirred for at least 1 day to remove the excess of copper(II) ions by complex formation. Removal of copper(II) ions is very important if one wants to prevent the formation of copper(II) phthalocyanine in the subsequent cyclotetramerisation step. Next, the solution was filtered and the residue was washed thoroughly with dichloromethane. The organic layer was separated and washed with water. After the solvent underwent drying and evaporation, TLC showed that a mixture of three products was obtained, which was later identified as containing the desired dicyano compound, the mixed bromocyano product, and the starting dibromo compound. The separation of the various organic species was achieved by a chromatography column over silica gel with toluene as the eluent. Repeated crystallization from hexane led to the pure dicyano product. In general, the yield of the Rosenmund−Von Braun reaction was always lower than 60%.

The detailed synthetic procedure is described for 1,2-dicyano-4,5-bisdecyloxybenzene, but all the other substituted phthalonitriles were obtained in a similar way.

Synthesis of 1,2-Bis(decyloxy)benzene. Oxygen was removed from a mixture of catechol (0.2 mol, 22.0 g), 1-bromodecane (0.4 mol, 88.5 g), potassium hydroxide (0.4 mol, 26.5 g), and Aliquat 336 phase-transfer catalyst (1 mL) by repeated evacuation followed by admission of nitrogen. Next, the mixture was heated at 100 °C in a dry nitrogen atmosphere with stirring. After 8 h, 250 mL of water and 100 mL of dichloromethane were added. The organic layer was separated and the aqueous layer was extracted three times with 50 mL of diethyl ether. The combined organic layers were washed with 200 mL of water, dried over $MgSO_4$, and concentrated. The residue was crystallized from acetone. Yield: 80% (62 g). mp 41 °C. MS *m*/*z*: 390 (M^+). IR (KBr): 3000−2750 (alkyl), 1500 (aryl), 750 (*o*-substituted benzene) cm^{-1}. ^1H NMR (δ, $CDCl_3$): 0.88 (t, 6H, CH_3), 1.27 (m, 24H, CH_2), 1.80 (m, 4H, CH_2), 3.99 (t, 4H, OCH_2), 6.88 (s, 4H, Ar). CHN analysis: $C_{26}H_{46}O_2$ (390.64). Calcd (%): C, 79.94; H, 11.87. Found (%): C, 79.72; H, 11.84.

Synthesis of 1,2-Dibromo-4,5-bis(decyloxy)benzene. To a solution of 1,2-bis(decyloxy)benzene (0.05 mol, 20.0 g) in 100 mL of dichloromethane, a solution of bromine (0.10 mol, 5.1 mL) in 15 mL of dichloromethane was added over ca. 1 h, the first half at 0 °C and the second half at room temperature. The reaction mixture was stirred overnight at room temperature. Liberated HBr vapors were trapped in a concentrated NaOH solution. The reaction mixture was then washed with saturated $Na_2S_2O_5$, saturated $NaHCO_3$, and twice with water. The extract was dried over $MgSO_4$ and evaporated to dryness. Purification was done by crystallization from acetone. Yield: 92% (26 g). mp 42 °C. MS *m*/*z*: 548 (M^+). IR (KBr): 3000−2750 (alkyl), 1500 (aryl), 750 (*o*-substituted benzene) cm^{-1}. ^1H NMR (δ, $CDCl_3$): 0.88 (t, 6H, CH_3), 1.27 (m, 24H, CH_2), 1.77 (m, 4H, CH_2), 3.94 (t, 4H, OCH_2), 7.06 (s, 2H, Ar). CHN analysis: $C_{26}H_{44}O_2Br_2$ (548.43). Calcd (%): C, 56.94; H, 8.09. Found (%): C, 57.19; H, 8.16.

Synthesis of 1,2-Dicyano-4,5-bis(decyloxy)benzene. A mixture of 1,2-dibromo-4,5-bis(decyloxy)benzene (0.05 mol, 24.5 g) and CuCN (014 mol, 12.1 g) was heated at reflux in 100 mL of DMF for 6 h under a dry atmosphere of nitrogen. After being cooled to room temperature, the reaction mixture was poured into an aqueous ammonia solution (25%, 1 L) and stirred for 62 h. The mixture was filtered, the water phase extracted with dichloromethane, and the remaining solid poured into an aqueous ethylenediamine solution and stirred for 12 h. After filtration, the solid was washed with water, dissolved in dichloromethane, filtrated, and evaporated to dryness. The crude product was purified by column chromatography over silica (eluent: chloroform) and crystallized from hexane. Yield: 29% (5.3 g). mp 106 °C. MS *m*/*z*: 440 (M^+). IR (KBr): 2750−3000 (alkyl), 2240 (CN), 1500 (aryl), 750 (*o*-substituted benzene) cm^{-1}. ^1H NMR (δ, $CDCl_3$): 0.88 (t, 6H, CH_3), 1.27 (m, 24H, CH_2), 1.86 (m, 4H, CH_2), 4.05 (t, 4H, OCH_2), 7.11 (s, 2H, Ar). CHN analysis: $C_{28}H_{44}O_2N_2$ (440.66). Calcd (%): C, 76.32; H, 10.06; N, 6.36. Found (%): C, 76.18; H, 10.05; N, 6.19.

A mixture of 1,2-dicyano-4,5-bis(decyloxy)benzene (2.27 mmol, 1.00 g), erbium(III) acetate (0.30 mol, 135.3 mg), and 1,8-diazabicyclo[5.4.0]undec-7-ene (1.3 mmol, 0.05 mL) was stirred in 1-hexanol (6 mL) at reflux for 20 h. After the mixture cooled to room temperature and evaporated to dryness, the green residue was dissolved in a minimum amount of chloroform and the product was precipitated in methanol and filtered. After evaporation to dryness, the green residue was dissolved in a few milliliters of chloroform and reprecipitated by addition of methanol. The crude product was purified by chromatography on silica and size exclusion chromatography on Bio-Rad Bio-Beads S-X3 (eluent: chloroform). The green (neutral) fractions were collected. Yield: 24%. MS *m*/*z*: 3669 (M^+). UV/vis: ($CHCl_3$) λ_{max}/nm: 682, 612, 495, 370.

3. Results and Discussion

The sandwich complexes containing lanthanide ions were prepared by a template reaction of four phthalonitrile precursors with the corresponding lanthanide ion (Scheme 1). The reaction consisted of thoroughly mixing the disubstituted phthalonitrile (1,2-dicyano-5,4-bis-alkoxybenzene) with 1/8 equiv of a lanthanide(III) acetate salt, and to heat the mixture at 150 °C for 20 hours in the presence of 1/2 equiv of 1,8-diazabicyclo-[5.4.0]undec-7-ene (DBU) in 1-hexanol.[6] After cooling to room temperature, the mixture was dissolved in a minimum amount of chloroform and the product was precipitated in methanol and filtered. The purification of the reaction mixture consisted of multiple-step column chromatography over silica gel using chloroform as the eluent, followed by size exclusion chromatography on Bio-Rad Bio-Beads S-X3 as the eluent and crystallization from ethyl acetate. During column chromatography, two bands (blue and green) eluted from the column, but only the green fraction was collected (cation radical). The purity of the lanthanide complexes was checked by MALDI-TOF and UV/vis spectroscopy. Purification proceeded to the point where liquid chromatography resulted in one single band (or one spot on TLC), of which the UV/vis spectrum was consistent with that of a double-decker. In Table 1, an overview of the complexes, and their MALDI-TOF analysis data, is given. Compounds with the large lanthanide ions (at the beginning of the lanthanide series) were much more difficult to obtain than the compounds of the lanthanides at the end of the series. This may partially explain why most of the studies on bis(phthalocyaninato)lanthanide complexes were focused in the past on the lutetium(III) complexes. All the lanthanide complexes were obtained as dark green compounds.

All the investigated compounds showed a viscous mesophase over a wide temperature range (>100 °C). The derivatives with a chain length shorter than $C_8H_{17}O$ decomposed before the clearing point was reached. Only one type of mesophase has been detected. The optical textures, observed by polarizing optical microscopy, were typical of that of a columnar mesophase showing both large cylindrical domains and large homeotropic area, suggesting strongly a hexagonal

Table 1. MALDI-TOF Results of the $[(C_nH_{2n+1}O)_8Pc]_2Ln$ Complexes

compound	formula	*M* (isotopic)	*M* (found)
$[(C_{12}H_{25}O)_8Pc]_2Pr$	$C_{256}H_{416}O_{16}N_{16}Pr$	4112.1	4111.4
$[(C_{12}H_{25}O)_8Pc]_2Nd$	$C_{256}H_{416}O_{16}N_{16}Nd$	4113.1	4114.8
$[(C_{12}H_{25}O)_8Pc]_2Eu$	$C_{256}H_{416}O_{16}N_{16}Eu$	4124.1	4123.2
$[(C_{12}H_{25}O)_8Pc]_2Gd$	$C_{256}H_{416}O_{16}N_{16}Gd$	4129.1	4128.9
$[(C_{12}H_{25}O)_8Pc]_2Tb$	$C_{256}H_{416}O_{16}N_{16}Tb$	4130.1	4129.8
$[(C_{12}H_{25}O)_8Pc]_2Dy$	$C_{256}H_{416}O_{16}N_{16}Dy$	4135.2	4135.6
$[(C_{12}H_{25}O)_8Pc]_2Ho$	$C_{256}H_{416}O_{16}N_{16}Ho$	4136.2	4136.5
$[(C_{12}H_{25}O)_8Pc]_2Er$	$C_{256}H_{416}O_{16}N_{16}Er$	4137.2	4137.5
$[(C_{12}H_{25}O)_8Pc]_2Tm$	$C_{256}H_{416}O_{16}N_{16}Tm$	4140.2	4139.5
$[(C_{12}H_{25}O)_8Pc]_2Yb$	$C_{256}H_{416}O_{16}N_{16}Yb$	4145.2	4145.9
$[(C_{12}H_{25}O)_8Pc]_2Lu$	$C_{256}H_{416}O_{16}N_{16}Lu$	4146.2	4146.8
$[(C_4H_9O)_8Pc]_2Er$	$C_{128}H_{160}O_{16}N_{16}Er$	2343.2	2341.1
$[(C_5H_{11}O)_8Pc]_2Er$	$C_{144}H_{192}O_{16}N_{16}Er$	2567.4	2567.9
$[(C_6H_{13}O)_8Pc]_2Er$	$C_{160}H_{224}O_{16}N_{16}Er$	2791.7	2792.8
$[(C_8H_{17}O)_8Pc]_2Er$	$C_{192}H_{288}O_{16}N_{16}Er$	3240.2	3241.1
$[(C_9H_{19}O)_8Pc]_2Er$	$C_{208}H_{320}O_{16}N_{16}Er$	3464.4	3466.1
$[(C_{10}H_{21}O)_8Pc]_2Er$	$C_{224}H_{352}O_{16}N_{16}Er$	3668.7	3668.8
$[(C_{12}H_{25}O)_8Pc]_2Er$	$C_{256}H_{416}O_{16}N_{16}Er$	4137.2	4137.5
$[(C_{14}H_{29}O)_8Pc]_2Er$	$C_{288}H_{480}O_{16}N_{16}Er$	4585.7	4583.4
$[(C_{15}H_{31}O)_8Pc]_2Er$	$C_{304}H_{512}O_{16}N_{16}Er$	4809.9	4808.6
$[(C_{16}H_{33}O)_8Pc]_2Er$	$C_{320}H_{544}O_{16}N_{16}Er$	5034.2	5032.7
$[(C_{18}H_{37}O)_8Pc]_2Er$	$C_{352}H_{608}O_{16}N_{16}Er$	5482.7	5478.7

Table 2. Mesophase Behavior of the $[(C_nH_{2n+1}O)_8Pc]_2Er$ Complexes

compound	transition temperatures[a] (°C)
$[C_4H_9O)_8Pc]_2Er$	Cr 202 Col_h >280 Dec
$[C_5H_{11}O)_8Pc]_2Er$	Cr 174 Col_h >280 Dec
$[C_6H_{13}O)_8Pc]_2Er$	Cr 147 Col_h >280 Dec
$[C_8H_{17}O)_8Pc]_2Er$	Cr 137 Col_h 263 I
$[C_9H_{19}O)_8Pc]_2Er$	Cr 93 Col_h 239 I
$[C_{10}H_{21}O)_8Pc]_2Er$	Cr 71 Col_h 180 I
$[C_{12}H_{25}O)_8Pc]_2Er$	Cr 68 Col_h 174 I
$[C_{14}H_{29}O)_8Pc]_2Er$	Cr 58 Col_h 180 I
$[C_{15}H_{31}O)_8Pc]_2Er$	Cr 44 Col_h 170 I
$[C_{16}H_{33}O)_8Pc]_2Er$	Cr 43 Col_h 163 I
$[C_{18}H_{37}O)_8Pc]_2Er$	Cr 65 Col_h 151 I

[a] Cr = crystalline phase; Col_h = hexagonal columnar mesophase; Dec. = decomposition; I = isotropic liquid.

Table 3. Mesophase Behavior of the $[(C_{12}H_{25}O)_8Pc]_2Ln$ Complexes

compound	transition temperatures[a] (°C)
$[C_{12}H_{25}O)_8Pc]_2Pr$	Cr 74 Col_h 208 I
$[C_{12}H_{25}O)_8Pc]_2Nd$	Cr 66 Col_h 206 I
$[C_{12}H_{25}O)_8Pc]_2Eu$	Cr 65 Col_h 203 I
$[C_{12}H_{25}O)_8Pc]_2Gd$	Cr 68 Col_h 218 I
$[C_{12}H_{25}O)_8Pc]_2Tb$	Cr 72 Col_h 205 I
$[C_{12}H_{25}O)_8Pc]_2Dy$	Cr 83 Col_h 205 I
$[C_{12}H_{25}O)_8Pc]_2Ho$	Cr 85 Col_h 190 I
$[C_{12}H_{25}O)_8Pc]_2Er$	Cr 68 Col_h 174 I
$[C_{12}H_{25}O)_8Pc]_2Tm$	Cr 68 Col_h 182 I
$[C_{12}H_{25}O)_8Pc]_2Yb$	Cr 84 Col_h 192 I
$[C_{12}H_{25}O)_8Pc]_2Lu$	Cr 92 Col_h 188 I

[a] Cr = crystalline phase; Col_h = hexagonal columnar mesophase; I = isotropic liquid.

columnar mesophase (Col_h). The transition temperatures of the compounds of the two series are listed in Tables 2 and 3. Both the melting and clearing temperatures were found to decrease with increasing chain length (Table 2), though this decrease is faster for the first homologues of the series ($n \leq 10$) and then very smooth afterward. Notwithstanding, a reduction of the melting and clearing temperatures by 130−140 °C was nevertheless achieved from the butyloxy compound to the octadecyloxy derivative. Still, the mesomorphic temperature range was not affected by chain extension and remained quite constant for the whole series (Figure 2). As for the effect of the metal, the lanthanide ion has a much less pronounced influence on the transition temperatures, and only a slight narrowing of the mesophase temperature range (essentially due to the depression of the clearing temperature) is observed from the light lanthanide ions to the heavy ones (Table 3, Figure 3). This is in striking contrast to lanthanide(III) alkanoates,[19] and Schiff's base complexes with nitrate counterions for which either the mesophase stability was considerably decreased or the liquid-crystalline properties totally suppressed, going along the lanthanide series from La to Lu.[20] A likely explanation for

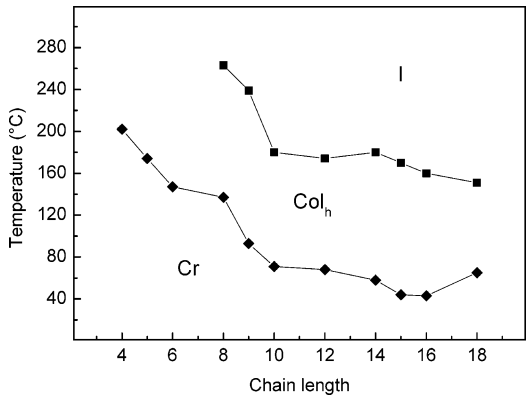

Figure 2. Influence of the alkoxy chain length on the transition temperatures of the $[(C_nH_{2n+1}O)_8Pc]_2Er$ complexes.

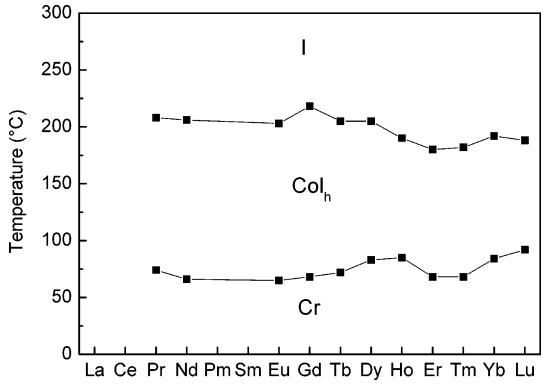

Figure 3. Influence of the lanthanide ion on the transition temperatures of the $[(C_{12}H_{25}O)_8Pc]_2Ln$ complexes.

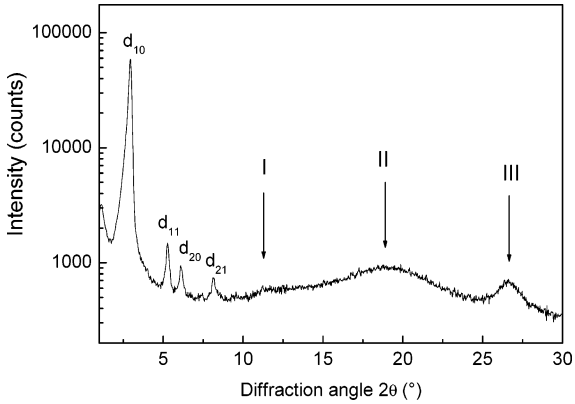

Figure 4. X-ray diffractogram of $[(C_{10}H_{21}O)_8Pc]_2Er$ at 150 °C, in the hexagonal columnar mesophase.

(19) Binnemans, K.; Jongen, L.; Görller-Walrand, C.; D'Olieslager, W.; Hinz, D.; Meyer, G. *Eur. J. Inorg. Chem.* **2000**, 1429.
(20) Binnemans, K.; Van Deun, R.; Bruce, D. W.; Galyametdinov, Yu. G. *Chem. Phys. Lett.* **1999**, *300*, 509.

Table 4. X-ray Characterization of the Erbium Complexes, $[(C_nH_{2n+1}O)_8Pc]_2Er$, at Various Temperatures[a]

T (°C)	d_{obs} (Å)	I	hk	d_{calc} (Å)	a (Å)	S (Å^2)	T (°C)	d_{obs} (Å)	I	hk	d_{calc} (Å)	a (Å)	S (Å^2)
						$n = 6$: Cr 147 Col_h > 280 Dec.							
150	24.5	VS	10	24.45	28.25	690	200	24.35	VS	10	24.35	28.1	685
	14.1	S	11	14.1				14.0	S	11	14.0		
	12.25	S	20	12.2				12.15	S	20	12.15		
	9.25	M	21	9.25				9.25	M	21	9.2		
	7.5	br	I					7.4	br	I			
	4.5	br	II					4.6	br	II			
	3.5	sh	III					3.5	sh	III			
						$n = 8$: Cr 137 Col_h 263 I							
150	25.8	VS	10	25.8	29.8	769	200	24.7	VS	10	24.8	28.6	710
	14.9	S	11	14.9				14.3	S	11	14.3		
	12.9	S	20	12.9				12.5	S	20	12.4		
	9.8	M	21	9.75				9.35	M	21	9.4		
	7.6	br	I					7.5	br	I			
	4.5	br	II					4.6	br	II			
	3.5	sh	III					3.5	sh	III			
						$n = 9$: Cr 93 Col_h 239 I							
100	27.5	VS	10	27.5	31.75	873	200	26.3	VS	10	26.3	30.35	799
	15.85	S	11	15.9				15.25	S	11	15.2		
	13.7	S	20	13.75				13.15	S	20	13.15		
	10.35	M	21	10.4				9.9	M	21	9.95		
	7.6	br	I					7.4	br	I			
	4.5	br	II					4.6	br	II			
	3.5	sh	III					3.5	sh	III			
150	27.3	VS	10	27.2	31.4	854							
	15.7	S	11	15.7									
	13.6	S	20	13.6									
	10.3	M	21	10.3									
	7.5	br	I										
	4.5	br	II										
	3.5	sh	III										
						$n = 10$: Cr 71 Col_h 180 I							
100	28.1	VS	10	28.1	32.45	912	150	27.9	VS	10	27.95	32.3	902
	16.25	S	11	16.2				16.15	S	11	16.1		
	14.1	S	20	14.05				14.0	S	20	14.0		
	10.6	M	21	10.6				10.5	M	21	10.55		
	7.5	br	I					7.5	br	I			
	4.5	br	II					4.6	br	II			
	3.5	sh	III					3.4	sh	III			
						$n = 12$: Cr 68 Col_h 174 I							
100	30.0	VS	10	30.0	34.65	1039	150	29.4	VS	10	29.4	33.95	998
	17.35	S	11	17.3				16.9	S	11	17.0		
	15.0	S	20	15.0				14.8	S	20	14.7		
	11.35	M	21	11.35				11.1	M	21	11.1		
	7.6	br	I					7.5	br	I			
	4.5	br	II					4.5	br	II			
	3.5	sh	III					3.5	sh	III			
						$n = 14$: Cr 58 Col_h 180 I							
100	31.3	VS	10	31.15	36.0	1120	150	30.8	VS	10	30.8	35.6	1095
	17.9	S	11	18.0				17.7	S	11	17.8		
	15.6	S	20	15.6				7.5	br	I			
	7.6	br	I					4.5	br	II			
	4.5	br	II					3.5	br	III			
	3.5	br	III										
						$n = 15$: Cr 44 Colh 170 I							
100	32.2	VS	10	32.2	37.2	1197	150	31.2	VS	10	31.2	36.0	1124
	18.6	S	11	18.6				18.0	S	11	18.0		
	16.15	S	20	16.1				15.6	S	20	15.6		
	7.6	br	I					7.5	br	21			
	4.5	br	II					4.5	br	I			
	3.5	br	III					3.5	br	II			
										III			
						$n = 16$: Cr 43 Col_h 163 I							
100	32.6	VS	10	32.6	37.6	1227	150	32.1	VS	10	32.0	36.95	1182
	18.7	S	11	18.8				18.45	S	11	18.5		
	16.25	S	20	16.3				15.95	S	20	16.0		
	7.6	br	I					7.4	br	I			
	4.5	br	II					4.5	br	II			
	3.5	br	III					3.5	br	III			
						$n = 18$: Cr 65 Col_h 151 I							
100	33.9	VS	10	33.95	39.2	1331							
	19.65	S	11	19.6									
	16.95	S	20	17.0									
	7.6	br	I										
	4.5	br	II										
	3.5	sh	III										

[a] d_{obs} and d_{calc} are the observed and calculated d-spacings, respectively; I is the intensity of the diffraction signal (VS, very strong; S, strong; M, medium; W, weak; VW, very weak; br, broad; sh, shoulder). hk is the indexation of the two-dimensional lattice; I, II and III are halos; a is the lattice parameter; and S is the lattice area of the hexagonal columnar phase (Col_h−$p6mm$).

this behavior can lie in the fact that here the lanthanide ions are hidden and sandwiched between the two phthalocyanine rings, limiting as such possible additional specific interactions with neighboring molecules; the columnar behavior is clearly governed by the phthalocyanine, the metals simply acting as a perturbation. Let us however recall that a quite different conclusion was drawn for the related alkythio-substituted phthalocyanine sandwich complexes of Eu^{III}, Tb^{III}, and Lu^{III}. Indeed, a small metal dependency was evidenced, with the overall decrease of both transition temperatures from Eu^{III} to Lu^{III}, but more evident was the continuous decrease of the clearing temperature with chain extension from 220 to 250 °C for $n = 8$ to 110−130 °C for $n = 18$, and the consequent narrowing of the mesomorphic temperature ranges.[10]

The mesophase was identified as a hexagonal columnar mesophase (Col_h) by small-angle X-ray diffraction. For each compound, and when possible, a diffraction pattern was recorded at four different temperatures, that is, 50, 100, 150, and 200 °C, to ascertain the presence of a single mesophase only within the mesomorphic domain. The columnar polymorphism (Col_r and Col_h) claimed by other authors for the $[(C_nH_{2n+1}O)_8Pc]_2Lu$ compounds was not detected here.[9,10]

In Figure 4, the X-ray diffractogram of $[(C_{10}H_{21}O)_8Pc]_2Er$ in the mesophase at 150 °C is given as a representative example since all the lanthanide complexes showed exactly the same features. The indexation of the diffractogram is summarized in Table 4. In the small-angle region up to four sharp Bragg reflections with the $1:\sqrt{3}:\sqrt{4}:\sqrt{7}$ reciprocal spacings ratio were observed, typical for a 2D hexagonal lattice and corresponding to the indexation $(hk) = (10)$, (11), (20), and (21). In the wide-angle region, three halos were observed corresponding to short interactions within the columns. First, at ca. 7.5−7.8 Å, a very weak halo (I) could be seen, likely corresponding to the thickness of the bis(macrocyclic) complex, which was assigned to the loose and short-range stacking distance of the double-decker. Then we observed the diffuse and broad halo (II) centered at around 4.6 Å, which reflects the liquidlike order of the molten aliphatic chains. Finally, a less broad halo, (III), sometimes quite sharp, was also systematically observed at around 3.4−3.5 Å, which may be related to the regular stacking distance between two successive phthalocyanine cores. This latter stacking distance is a bit surprising here on account of the double-decker structure of the complexes and can be attributed to either intermacrocyclic spacing uncorrelated to the position of the lanthanide ion, that is, single-decker species, or to rapid thermal fluctuations which extinguish the differences between the upper and lower macrocycles in the sandwich compound, that is, the repeat distance between two cofacially stacked phthalocyanine disks. The former explanation implies dephasing introduced by monocyclic impurities according to a periodic model.[6] As for thermal fluctuations, they are strongly encouraged by the radical nature of the sandwich complex. Indeed, one of the phthalocyanine rings bears an unpaired electron and as such is not aromatic and thus not flat. Consequently, this structural asymmetry forces trampoline-like movements of the phthalocyanine rings,[10] which on increasing the temperature, may occur faster to give apparent single-deckers on the time average. Figure 5 shows that the halo III becomes less intense and shifts to smaller diffraction angles with increasing temperature, which indicates an increasing disorder along the columnar structure as the temperature is raised. This latter observation is more in favor with the second hypothesis than with the first explanation. The results of these investigations are summarized in Tables 4 and 5.

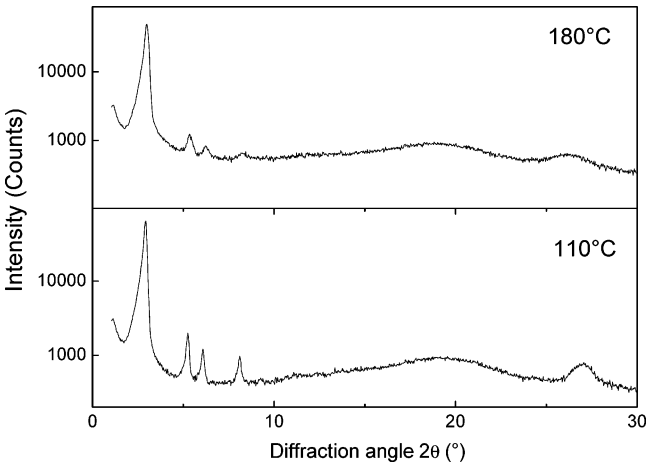

Figure 5. Temperature dependence of the X-ray diffractograms of $[(C_{10}H_{21}O)_8Pc]_2Er$.

To obtain a better understanding of the overall behavior and organization in the mesophase of such double-deckers, the variation of the parameter S was followed as a function of the chain length (erbium series). As expected, the columnar cross-sectional area varies almost linearly with the incremental number of methylene groups (Figure 6). Moreover, it showed little dependence with the temperature. In fact, one can observe a small decrease of the columnar cross section by less than 5% for a temperature variation of 50 °C, and by less than 10% over a temperature range of 100 °C. The molecular volume increasing with temperature, this slight contraction is due to the thermal expansion of the complex which occurs preferentially in the direction parallel to the columnar axis, that is, the height of the sandwich increases, than within the hexagonal plane. This is also consistent with the shift of the halos I and III toward the small-angle region. Extrapolation to zero methylene groups gives a value of ca. 400 $Å^2$, which is in good agreement with the surface area of the rigid, aromatic phthalocyanine core. Thus, it appears that the double-deckers stack on top of each other to form columns, without tilting of the phthalocyanine rings. Due to thermal motions and to the staggered configuration of the two phthalocyanine rings forming the complex, the sandwich takes the shape of a cylinder with a circular cross section, in good agreement with the hexagonal symmetry of the phase. The influence of the lanthanide ion on the structural parameters a and S (Table 5), as well as their variation with temperature (Figure 7), is however not so clear. Due to the shielding of the ion sandwiched between the two phthalocyanine rings, important changes along the 4f series were not expected. This is true for most of the series starting from Ln = Nd, where the variation of S is negligible at 100 °C (S = ca. 1050 $Å^2$). However, at 150 °C, the variation of S is not more correlated with the nature of the

Table 5. X-ray Characterization of the Lanthanide Complexes $[(C_{12}H_{25}O)_8Pc]_2Ln$; Lattice Parameter *a* and Lattice Area *S* of the Hexagonal Columnar Phase Of the $[(C_{12}H_{25}O)_8Pc]_2Ln$ Complexes at Various Temperatures.

T (°C)	d_{obs} (Å)	*I*	*hk*	d_{calc} (Å)	*a* (Å)	*S* (Å²)	*T* (°C)	d_{obs} (Å)	*I*	*hk*	d_{calc} (Å)	*a* (Å)	*S* (Å²)	*T* (°C)	d_{obs} (Å)	*I*	*hk*	d_{calc} (Å)	*a* (Å)	*S* (Å²)
								Ln = Pr: Cr 74 Col_h 208 I												
100	28.7	VS	10	28.6	33.0	944	150	28.5	VS	10	28.4	32.8	940	200	28.0	VS	10	28.0	32.35	905
	16.5	S	11	16.5				16.35	S	11	16.4				16.15	S	11	16.15		
	7.6	br	I					7.6	br	I					7.5	br	I			
	4.5	br	II					4.6	br	II					4.6	br	II			
	3.5	sh	III					3.4	sh	III					3.5	sh	III			
								Ln = Nd: Cr 66 Col_h 206 I												
100	29.75	VS	10	29.7	34.3	1018	150	29.6	VS	10	29.6	34.2	1011	200	29.2	VS	10	29.15	33.65	981
	17.1	S	11	17.15				17.1	S	11	17.1				16.8	S	11	16.8		
	14.8	S	20	14.85				7.5	br	I					14.6	S	20	14.6		
	7.5	br	I					4.6	br	II					7.4	br	I			
	4.5	br	II					3.5	sh	III					4.6	br	II			
	3.5	sh	III												3.5	sh	III			
								Ln = Eu: Cr 65 Col_h 203 I												
100	30.1	VS	10	30.0	34.65	1039	150	29.9	VS	10	29.8	34.4	1025							
	17.3	S	11	17.3				17.2	S	11	17.2									
	15.0	S	20	15.0				14.9	S	I	14.9									
	7.4	br	I					7.5	br	II										
	4.5	br	II					4.5	br	III										
	3.5	sh	III					3.4	sh											
								Ln = Gd: Cr 68 Col_h 218 I												
100	29.9	VS	10	29.9	34.5	1032	150	30.0	VS	10	30.0	34.65	1039	200	27.9	VS	10	27.9	32.2	899
	17.3	S	11	17.25				17.3	S	11	17.3				16.15	S	11	16.1		
	14.95	S	20	14.95				15.0	S	20	15.0				13.9	S	20	13.95		
	11.3	M	21	11.3				11.4	M	21	11.3				7.4	br	I			
	7.5	br	I					7.4	br	I					4.6	br	II			
	4.5	br	II					4.5	br	II					3.5	sh	III			
	3.5	sh	III					3.5	sh	III										
								Ln = Tb: Cr 72 Col_h 205 I												
100	30.0	VS	10	30.0	34.65	1039	150	29.8	VS	10	29.75	34.35	1022	200	29.0	VS	10	29.0	33.5	971
	17.25	S	11	17.3				17.15	S	11	17.15				16.7	S	11	16.75		
	15.1	S	20	15.0				14.9	S	20	14.9				7.4	br	I			
	7.6	br	I					7.5	br	I					4.6	br	II			
	4.5	br	II					4.5	br	II					3.5	sh	III			
	3.5	sh	III					3.5	sh	III										
								Ln = Dy: Cr 83 Col_h 205 I												
100	30.1	VS	10	30.1	34.75	1046	150	30.1	VS	10	30.15	34.8	1050	200	29.9	VS	10	29.9	34.5	1032
	17.35	S	11	17.4				17.4	S	11	17.4				17.25	S	11	17.25		
	15.1	S	20	15.05				15.1	S	20	15.1				15.0	S	20	14.95		
	11.4	M	21	11.4				11.4	M	21	11.4				11.25	M	21	11.3		
	7.6	br	I					7.5	br	I					7.4	br	I			
	4.5	br	II					4.5	br	II					4.6	br	II			
	3.5	sh	III					3.5	sh	III					3.5	sh	III			
								Ln = Ho: Cr 85 Col_h 190 I												
100	30.6	VS	10	30.6	35.3	1081	150	30.25	VS	10	30.25	34.9	1057							
	17.6	S	11	17.7				17.45	S	11	17.45									
	15.3	S	20	15.3				15.1	S	20	15.15									
	7.6	br	I					11.45	M	21	11.45									
	4.6	br	II					7.4	br	I										
	3.5	sh	III					4.5	br	II										
								Ln = Tm: Cr 68 Col_h 182 I												
100	30.1	VS	10	30.2	34.9	1053	150	28.7	VS	10	28.7	33.15	951							
	17.4	S	11	17.45				16.6	S	11	16.6									
	15.1	S	20	15.1				7.5	br	I										
	11.4	M	21	11.4				4.5	br	II										
	7.6	br	I					3.5	sh	III										
	4.5	br	II																	
	3.5	sh	III																	
								Ln = Yb: Cr 84 Col_h 192 I												
100	30.1	VS	10	30.1	34.75	1046	150	28.4	VS	10	28.4	32.8	931							
	17.3	S	11	17.4				16.4	S	11	16.4									
	15.1	S	20	15.05				14.15	S	20	14.2									
	7.6	br	I	I				7.5	br	I										
	4.5	br	II	II				4.5	br	II										
	3.5	sh	III	III				3.5	sh	III										
								Ln = Lu: Cr 92 Col_h 188 I												
100	30.4	VS	10	30.3	35.0	1060	150	28.9	VS	10	28.9	33.4	964							
	17.4	S	11	17.5				16.7	S	11	16.7									
	15.2	S	20	15.15				14.4	S	20	14.45									
	11.5	M	21	11.45				10.9	M	21	10.9									
	7.5	br	I					7.5	br	I										
	4.5	br	II					4.5	br	II										
	3.5	sh	III					3.5	sh	III										

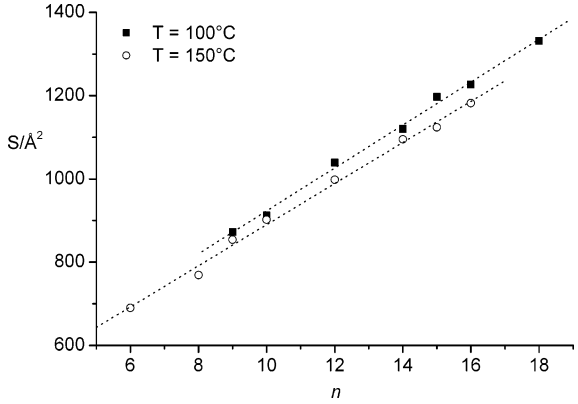

Figure 6. Variation of the columnar cross section as a function of chain length in the erbium series $[(C_nH_{2n+1}O)_8Pc]_2Er$.

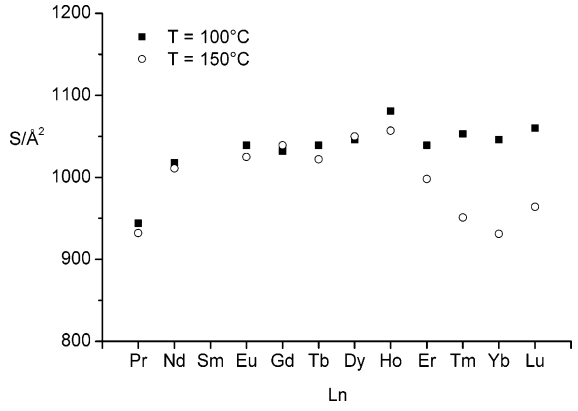

Figure 7. Variation of the columnar cross section as a function of the lanthanide ion $[(C_{12}H_{25}O)_8Pc]_2Ln$.

lanthanide ion, and for the complexes with Ln = Nd−Ho, a perfect invariance of the cross section was observed, while for the last four members of the series (Ln = Er, Tm, Yb, Lu), *S* drops down to ca. 900 Å^2. This sudden fall may be connected to the close proximity of the isotropic liquid since the clearing temperatures (and the mesomorphic temperature range) of these last four complexes are smaller than those of the other homologues of the series. The cohesion of the columns may also be weakened by the size of the ion.

For potential applications, the precise alignment of molecules at the interface with a substrate is an important parameter to control. To obtain insight into the two-dimensional ordering of such sandwich complexes in contact with a substrate, the orientational behavior of the erbium sandwich ($[C_{12}H_{25}O)_8Pc]_2Er$) was investigated at room temperature at the liquid (1-phenyloctane)/solid (graphite) interface by means of scanning tunneling microscopy (STM) and compared with that of a metal-free alkyl-substituted phthalocyanine $(C_{12}H_{25}O)_8PcH_2$. The ordering of the molecules on the graphite substrate does not necessarily reflect the ordering of the molecules within the mesophase due to the interaction with the support. Moreover, the images obtained are from a monolayer. However, these experiments illustrate at the molecular level in real space the preferred relative ordering of these molecules in a plane and are in agreement, taking into account the limitations discussed above, with the ordering proposed in the mesophase. The STM images of $(C_{12}H_{25}O)_8PcH_2$ are characterized by a pattern (nearly 6-fold symmetry or sometimes 4-fold symmetry) of bright structures which can be attributed to the location of the phthalocyanine units.[21] They appear as bright spots with 4-fold symmetry with a dark "hole", typical for metal-free phthalocyanines.[22] The contribution of the phthalocyanines to the tunneling current dominates the contrast. The darker parts correspond to the location of the alkyl chains, which however are not well-resolved. This might indicate that they are not completely immobilized on the substrate, in contrast to the phthalocyanine rings. The minimum distance between the cores of two adjacent molecules is approximately 3.0 nm, which indicates that the molecules are lying flat on the surface and that the alkyl chains of neighboring molecules are interdigitated, although their precise orientation cannot be determined.

Interestingly, the sandwich compound forms monolayers at the liquid/solid interface. Bright disks, attributed to the nonalkyl part of the molecules, are visible on a darker background. The alkyl chains are adsorbed in the dark background region but the lack of resolution indicates chain mobility. The ordering is not uniform but locally the molecules are organized with a nearly 6-fold symmetry. In those areas, the core-to-core distance in all directions is 3.0 nm (which is about 10% smaller than the value determined in bulk by X-ray diffraction), but very similar to the distance between $(C_{12}H_{25}O)_8PcH_2$ molecules. Sometimes, defects associated with the lack of a molecule are observed. The data show that the disks are in a side-on position with the Pc units parallel to the graphite substrate. The quality of the images is clearly lower compared to those of $(C_{12}H_{25}O)_8PcH_2$. The bright structures, attributed to the location of the Pc rings, do not show any fine structure, except for the appearance of streaky features parallel to the fast scan direction (horizontal: from left to right), indicating that the tip often "touches" the molecules. This illustrates the fact that the height of the sandwich molecules is considerably higher than those of the phthalocyanine ligands (the stacking distance in a columnar face is on the order of 0.65−0.70 nm). The lack of fine structure in the bright disks could be due to some (rotational) mobility of the phthalocyanine disks or might be caused by electronic effects caused by the presence of the lanthanide ion, which is the subject of continuing research.

4. Conclusions

The alkoxy-substituted bis(phthalocyaninato)lanthanide(III) complexes $[(C_nH_{2n+1}O)_8Pc]_2Ln$ were obtained as dark green solid compounds. The synthesis proved to be more difficult for the compounds with large lanthanide ions (beginning of the lanthanide series) than for the smaller ions at the end of the lanthanide series. All the complexes exhibit a hexagonal columnar mesophase (Col_h) over wide temperature ranges, whatever the chain length or the lanthanide ion. However, the transition temperatures were found to be chain-length-

(21) Qiu, X.; Chen, W.; Zeng, Q.; Xu, B.; Yin, S.; Wang, H.; Xu, S.; Bai, C. *J. Am. Chem. Soc.* **2000**, *122*, 5550.
(22) Freund, J.; Probst, O.; Grafstroem, S.; Dey, S.; Kowalski, J.; Neumann, R.; Woertge, M.; zu Pulitz. G. *J. Vac. Sci. Technol. B* **1994**, *12*, 1914.

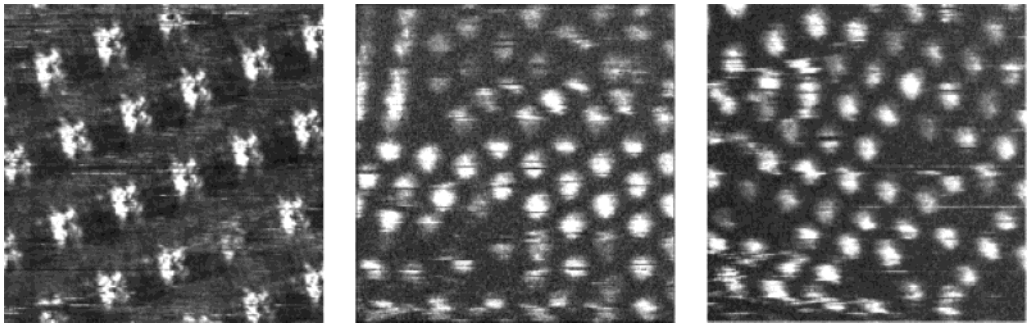

Figure 8. STM images of physisorbed monolayers at room temperature at the liquid (1-phenyloctane)/solid (HOPG) interface of (a) $(C_{12}H_{25}O)_8Pc$ (image size is 13.5 × 13.5 nm; $I_t = 0.25$ nA, $V_{bias} = -0.4$ V) and (b, c) $[(C_{12}H_{25}O)_8Pc]_2Er$ (image size is 24.0 × 24.0 nm; $I_t = 0.43$ nA, $V_{bias} = -1.1$ V).

dependent rather than lanthanide-dependent, unlike other mesomorphic lanthanide complexes, decreasing with extension of the chain but being overall constant for different lanthanide ions. On a graphite substrate, it has been shown that the sandwich molecules are in the side-on position.

Acknowledgment. K.B. and S.D.F. thank the F.W.O.-Flanders (Belgium) for a Postdoctoral Fellowship. J.S. is indebted to the "Flemish Institute for the Encouragement of Scientific and Technological Research in the Industry (IWT)" for financial support. He thanks the F.W.O.-Flanders for a travel grant. Financial support by the K.U. Leuven (GOA 03/3) and by the F.W.O.-Flanders (G.0117.03) is acknowledged. MALDI-TOF mass spectra were measured by G. Baggerman (K.U. Leuven) and CHN microanalyses by P. Bloemen (K.U. Leuven).

CM034236O